

Multi-Criteria Evaluation (MCE) of Groundwater Prospect and Vulnerability Index Mapping from Second-Order Geo-Electric Indices: A Case Study of Coastal Environments

Stanley Uchechukwu Eze^{*1}, Ekom E. Essien², Okiotor M. Edirin³, Sampson Jaja William⁴, Saleh A. Saleh⁵, Bello A. Maruff⁵, Ugwu Joshua Udoka⁶

¹*Department of Earth Sciences, Federal University of Petroleum Resources, Effurun, Nigeria

²Africa Centre of Excellence in Oilfield Chemical Research, University of Port Harcourt, Nigeria

³Department of Marine Geology, Nigeria Maritime University, Okerenkoko, Warri South, Delta State, Nigeria

⁴Department of Geology, University of Port Harcourt, Rivers State, Nigeria

⁵Department of Petroleum Engineering and Geosciences, Petroleum Training Institute, Effurun, Nigeria

⁶Department of Physics, Michael Okpara University of Agriculture Umudike, Abia State, Nigeria

*Corresponding author: uchechukwueze2014@gmail.com, ORCID iD: 0000-0003-0953-0609

doi: <https://doi.org/10.37745/bjesr.2013/vol11n589120>

Published December 26, 2023

Citation: Eze S.U., Essien E.E., Edirin O.M., William S.J., Saleh S.A., Maruff B.A., Ugwu J.U. . (2023) Multi-Criteria Evaluation (MCE) of Groundwater Prospect and Vulnerability Index Mapping from Second-Order Geo-Electric Indices: A Case Study of Coastal Environments, *British Journal of Earth Sciences Research*, 11 (5),89-120

ABSTRACT: *Exploration, management, and conservation of groundwater resources are critical stages toward potable water supply, driven by an expanding populace and the threat of a new norm posed by the distinctive coronavirus (COVID-19) pandemic. An in-depth assessment of the potential of groundwater reserves and susceptibility, using a multi-criteria evaluation, is required to aid in the planning of exploration programs for groundwater well location. Thirty (30) vertical electrical soundings (VES) were collected in Okerenkoko, Warri-Southwest, Delta State, to assess groundwater potential and vulnerability indicators. The VES data were used to obtain the first-order geoelectric variables, which were further exploited to calculate the geo-hydraulic parameters (hydraulic conductivity and transmissivity) and the vulnerability indices of the aquifer. For aquifer vulnerability appraisal, the AVI (aquifer vulnerability index), GOD (groundwater occurrence, overlying lithology, and depth to the aquifer), and GLSI (geoelectric layer susceptibility index) models were used. The groundwater characteristics in the area were evaluated using the aquifer resistivity, thickness, transmissivity and coefficient of anisotropy values of the aquifer layers defined from VES 1-30. The results show that aquifer layers with low resistivity favor more saturation due to immense porosity and therefore have greater groundwater potential than aquifers with high resistivity. The geoelectric structures defined by VES 1, 2 and 4 were consistent in their groundwater potential and yield judging from the multi-criteria*

assessments. The estimation of AVI, GOD, and GLSI models for aquifer threat assessment was facilitated by the multi-criteria evaluation of vulnerability indices utilizing hydro-geophysical parameters and index-based approaches. The models depend on the symbiotic effects of geologic array and thickness as the basis for the magnitude of conservation imparted to any particular aquifer involved. The AVI model map depicts that most of the VES locations were rated high (C between 1 and 2) to extremely high ($C < 1$), indicating that the aquifers at these locations are vulnerable to pollution. However, the extent of vulnerability observed in the GOD model is less than in the AVI model, as GOD accords much more inclination to the inherent properties of geologic entities. The GOD model map categorized the vulnerability index ratings in the area as negligible (0.0-0.1), low (0.1-0.3) and moderate (0.3-0.5), with most VES locations ranked low to moderate, which indicates that these locations are susceptible to vulnerability. In the GLSI model, individual overlying layer thicknesses were prioritized. The GLSI model map shows that the vulnerability index ratings in the area are ranked as moderate (2.00-2.99), high (3.00-3.99) and extremely high (≥ 4.00) with most of the VES locations ranked moderate to high with the exception of VES 27, which ranked extremely high in both AVI and GLSI indices. By correlating the results of vulnerability index valuation for the AVI, GOD and GLSI models, more correlation was observed between the AVI and GLSI models. These findings validate the adoption of a multi-criteria evaluation methodology for groundwater potential and aquifer vulnerability studies and are strongly recommended as practical criteria for locating subsurface aquifers and their protective measures for groundwater prospect development planning and management.

KEYWORDS: groundwater pollution, aquifer protection, vulnerability indices, avi, god and GlSI

INTRODUCTION

In groundwater production practice and management, it is vital to properly evaluate the aquifer properties of the area to have a precise definition of its groundwater potential zones. In rural, sub-urban, and metropolitan areas, groundwater constitutes one of the most important natural resources and a key source of water supply (Abija 2018). Access to edible water is an elemental prerequisite for human and economic evolution, because of its availability for drinking, domestic uses and farm irrigation for food production (Singh and Singh 2009). The recognition of the description and identification of subsurface situations favorable to groundwater occurrence is important in groundwater studies. The presence of porosity and permeability in the anchor rock supporting groundwater is an important determinant of its occurrence, quantity, and exploitability. These two requirements are essential to the extraction of groundwater (Chernicoff and Whitney 2009). Aquifer resistivity (ρ) and thickness (h) have been consistent as criteria of hydrogeological interest that can be used to assess groundwater inherent in an area (Rao and Briz-Kishore 1991), cited in Adiat et al. (2013). Aquifer resistivity and thickness (otherwise termed first-order geoelectric parameters) are the primary parameters obtained from geophysical inversion of vertical electrical sounding (VES) data. The hydraulic view of groundwater aquifers is most often predicted by

analysis of pumping test data or from the first-order geoelectric parameters using numerical equations (Abija et al. 2019).

Surface geophysical measurement is an inexpensive, rapid and noninvasive means of estimating aquifer hydraulic properties. Estimation of hydraulic conductivity (k) and transmissivity (Tr) allows for calculable indication of the hydraulic feedback of the aquifer to recharge and pumping and for discovering the groundwater possibility of an area (Abija et al. 2019). Evaluation of groundwater potential is usually a multi-criterion evaluation (MCE) process that relies on several parameters i.e. aquifer resistivity, aquifer thickness, transmissivity and coefficient of anisotropy to mention a few. While groundwater exploration and production are crucial, the current social demand emphasizes the need for groundwater resource vulnerability/protection. Vulnerability appraisal is a comprehensive and cardinal step in examining groundwater filth (Agoubi et al. 2018; Rizka 2018; George 2021a). The applicability of groundwater is most often defiled by leakage of leachate plumes from landfills, oil adulteration and dissipation water (from run-off/flood, toilets, oil-ceiling pipelines, and infected vessels) (Makeig 1982). This jeopardizes the fate of groundwater (Ugbaja and Edet 2004), signals for worry, and the demand to experimentally depict the regularly and cost-effectively usable hydrogeological system, largely those that are bound to culpability and vulnerability from superficial intrusions (Vu et al. 2021). The protectivity of groundwater assets is favored by the overlaying beds' of low permeability coefficient, thus giving limited or no passageway to fissures of pollutants. A number of techniques have been chartered and used in an analytical way to weigh the culpability of aquifers for pollution. A specific method has its rights and wrongs (George 2021b). Therefore, no familiar technique can be taken as the most applicable for a distinct setting (Foster et al. 2002). A few of the vulnerability evaluation techniques encompass unit longitudinal conductance (**S**), **DRASTIC** (depth to groundwater, recharge, aquifer type, soil properties, topography, impact of overburden zone and hydraulic conductivity) and confined and unconfined **GOD** (**G**=groundwater occurrence type, **O**=lithology of overlying layers and **D**=depth to the aquifer). While some of the procedures mentioned above are contingent on the hydraulic conductivity and thickness of the beds that lie above the aquifer, others are centered on the geo-electric characteristics of the layers that can be determined from geophysical field measurements and inversion. Longitudinal conductance (**S**), a Dar Zarrouk parameter is a known geophysical technique that identifies the vulnerability of the geo-electric layer(s) using their resistivity (ρ) and thickness (h) (Ugwu et al. 2016). Still, the results may be unresponsive to the presence of analogously high invulnerable geological lithology like laterites, which are admitted as favorable shielding intermediates for the concealed aquifers. In recent years, the use of other relative techniques such as the aquifer vulnerability index (**AVI**), **GOD**, and geo-electric layer susceptibility indexing (**GLSI**) in vulnerability appraisal is increasingly popular. The **AVI** model employs hydraulic resistance (**C**), which relies on hydraulic conductivity and the thickness of the aquifer protective layers (Stempvoort et al. 1993). The aquifer vulnerability index (**AVI**), in line with Stempvoort et al. (1993), is an approach that determines susceptibility by hydraulic resistance to vertical orientation of water loss through the protective beds. The **GOD-Index** model is a hydrogeological oriented method that evaluates aquifer vulnerability by multiplying the effect of

Publication of the European Centre for Research Training and Development -UK

three constants: groundwater existence (**G**), which considers the aquifer type confined or unconfined; overlying lithology to aquifer (**O**), which is a function of the layer resistivity and depth to the aquifer (**D**) (Oni et al. 2017). The **GLSI** model is a recently developed strategy that seeks to close the intrinsic imbalance between the longitudinal conductance (**S**) approach's insensitivity to the apparent presence of lateritic lithology and the **GOD** technique's over prioritization of the dominance of geologic units. By assigning index numbers to the layer thicknesses and layer resistivity weights, **GLSI** provides equal preference to overburden region thickness and projection of lithological units in aquifer vulnerability mapping (Oni et al. 2017).

According to Gogu and Dassaargues (2000) and Oni et al. (2017), the theories of **GOD** and **GLSI** are index-based parametric approaches that show a range of values related to a property, whereby each parameter defines the level of exposure to the pollution index. According to Stigter (2006), the best method for increasing certainty in vulnerability mapping is to compare the outcomes of different tools and analyze their consistency by conducting case studies on areas, where contamination occurred. As aforementioned, aquifer vulnerability assessment is a multi-criterion evaluation (MCE) process that relies on appraisals from several vulnerability indices.

The researched location, "Okerenkoko", in the kingdom of Gbaramatu, Warri, in the southern part of Delta State, where the renowned Nigerian Maritime University is situated, is an oil-producing community in the Niger Delta, plagued by environmental pollution and destruction from ongoing exploration and oil theft (bunkering) activity. Some of these oil splatters, whether they were done so knowingly or unknowingly, have the potential to leak into groundwater over time and impair it, and because of the stability of oil in water, this pollution can be extremely dangerous to the general public's health.

In a recent study by Okiator et al. (2022), the protective capacity of the aquifer in the study area was appraised employing the longitudinal conductance (**S**) method. The results showed areas with low, weak, good, very good, and excellent protective capacity based on the Oladapo and Akintorinwa (2007) protective capacity assessment. However, the S-model seems to amplify or misrepresent levels of contamination susceptibility more than the AVI, GOD and GLSI models. Therefore, this study re-assessed this area using a hydrogeological oriented model and a second-order geoelectric index-based parametric model to assess its groundwater potential and vulnerability index, as well as the feasibility of filtration from the contaminated water bodies. It is intended to define and classify formations vulnerable to surface or subsurface fluid.

Location and Geological Setting of the Study Area

Okerenkoko community is based within the Gbaramatu Kingdom within the Warri-South provincial government region of Delta State (Ijaw ethnic group). Okerenkoko is positioned between latitude 05°37'39.22" to 05°37'10.12"N and longitude 005°23'30.64" to 005°23'08.79"E. It is located inside the coastal waterways connecting Warri and Escravos, which are bounded by the Benin River and the Escravos River (Fig. 1). Rainforests and mangrove woodlands are what

define vegetation. The four oil-producing communities of Gbaramatu, Isaba, Ogbe-ijoh, and Oporoza constitute the Ijaw ethnic group politically. Some of the largest known oil and gas reserves in Delta State and the Niger Delta are located in this area. Here is where Nigeria Maritime University's main campus is located, along with a satellite campus at Kurutie community in the Gbaramatu Kingdom. Wealthy in common assets, this region has been tormented by asset shortages and community clashes for a long time. At one time or another the communities, have endured major oil spills, due to pipeline wrecks and other details, as they devour vegetation and aquatic life, which may influence ecosystems and groundwater (Amaize 2006). The nearby populace had once revolted against an oil spill alleged from a multinational oil giant's facility within the locale and contributed, among other things, to alleviation supplies, portable drinking water and a reasonable stipend to individuals for their misfortunes (Gbaramatu 2021). Warri South-West has an assessed land area of 1,722 km² (665 square miles) and is home to Delta State's Itsekiri and Ijaw ethnic bunches.

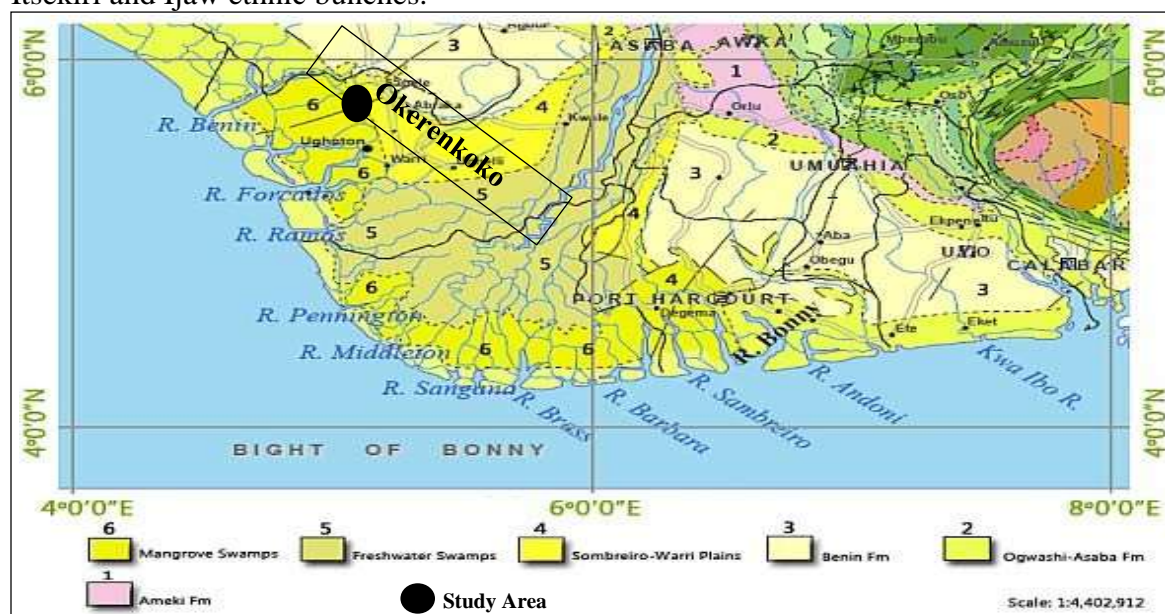


Fig. 1 Geological map of the Niger Delta region showing the areal dispersal of mangrove swamps and the Benin Formation (adapted from Nigeria Geological Survey Agency (NGSA 2004).

The region shares the same geology as the Niger Delta. Numerous researchers have studied the geology, stratigraphy, and structural framework of this area (Reyment 1965; Short and Stauble 1967; Asseez 1989). The Benin, Agbada, and Akata Formations are all included in the geological strata that make up the Niger Delta Basin. Reports from (e.g., Short and Stauble 1967; Doust and Omatsola 1990; Kulke 1995) provide brief descriptions of these formations' symbolic portions. Sea-level sand and shale layers make up the majority of the Akata Formation, and its subsoil is made up of dark gray sand and shale. The thickness of this stratum is assessed to be over 7,000 m (Doust and Omatsola 1990). The Upper Agbada Formation is a series of sandstone and shale

arrangements (Merki 1970). Essentially, it is made up of sand in the upper part and a small amount of shale in the lower part. Benin's upper strata, which are over 3,700 m thick, are frequently covered with lean layers of laterite of various thicknesses, but these layers are more obvious close to the coast.

Theoretical Concept of Vulnerability Indices Evaluation

The theoretical scheme in groundwater vulnerability evaluation is key to characterizing the safety of groundwater resources for groundwater monitoring and management programs. The following approaches to vulnerability index evaluation have been reported in the literature: aquifer vulnerability index (AVI), **GOD-index**, geoelectric layer susceptibility index (**GLSI**) and longitudinal conductance (**S**).

Aquifer Vulnerability Index (AVI)

According to Stempvoort et al. (1993), this method measures the vulnerability index of aquifers by hydraulic resistance to a vertical stream of water through the protecting layers. The computation of AVI utilizes two parameters: the thickness (h) of the defensive layers and the predicted hydraulic conductivity (K). Having computed the hydraulic conductivity (k), the hydraulic resistance (C) for the thickness (h_i) of each layer over the aquifer is computed as:

$$C = \sum_i^n \left(\frac{h_i}{k_i} \right) \quad (1)$$

where K_i is the hydraulic conductivity and h_i is the thickness of the overlying layers before the aquifer layer. Table 1 summarizes the link enclosed by the hydraulic resistance (C) and aquifer vulnerability index (AVI) and aids in deciding the susceptibility level.

Table 1 Relationship between aquifer vulnerability index (AVI) and hydraulic resistance (after Stempvoort et al. 1993)

Hydraulic Resistance (C)	Log C	Vulnerability index rating (AVI)
0-10	< 1	Extremely high
10-100	1-2.0	High
100-1000	2-3.0	Moderate
1000-10,000	3-4.0	Low
> 10,000	> 4.0	Extremely low

GOD-Index

According to Oni et al. (2017), **GOD** is an index-based aquifer vulnerability method where vulnerability is determined by multiplication of the effect of three constants: groundwater existence (**G**), which considers the aquifer type (artesian, confined or unconfined), overlying lithology to the aquifer (**O**) which is a function of the layer resistivity, and depth to the aquifer (**D**) (Oni et al. 2017), which is deliberated as:

$$\mathbf{GOD\ Index} = G \times O \times D \quad (2)$$

Each parameter in Eqn. (2) is assigned a characteristic index based on their model values.

Table 2 Attribution of notes for **GOD** index model parameters (after Khemiri et al. 2013).

Aquifer type (G)	Index	Overlying Lithology	Index	Depth to aquifer (m)	Index
Non-aquifer	0	< 60	0.4	< 2	1
Artesian	0.1	60-100	0.5	2-5	0.9
Confined	0.2	100-300	0.7	2-10	0.8
Semi- confined	0.3-0.5	300-600	0.8	10-20	0.7
Unconfined	0.6-1.0	> 600	0.6	20-50 50-100	0.6 0.5

This technique though not widely generalized, still stands as one of the best GIS-based index methods of vulnerability computation in a data-limited situation. One of the merits of the **GOD**-index method is that it considers the type of aquifer where groundwater occurs (artesian, confined or unconfined), keeping in mind that a confined aquifer (being overlain and underlain by impermeable layers) will be less vulnerable to contamination in the event of pollution compared to other types of aquifer. Therefore, it can be applied to any type of aquifer (except in karst regions), as each aquifer type is assigned an index based on Table 2. However, this method is only preferable in areas with wide differences in vulnerability.

Table 3 **GOD** parametric index rating (after Foster 1987)

Vulnerability class	Index rating
Negligible	0.0-0.1
Low	0.1-0.3
Moderate	0.3-0.5
High	0.5-0.7
Extreme	0.7-1.0

Tables 2 and 3 accord with the ascription of indices for **GOD** model amplitudes and the vulnerability classification indices.

Geoelectric Layer Susceptibility Index (GLSI)

GLSI is an explicit groundwater vulnerability computation method that employs the indices of geo-electric factors put together from the geoelectrical resistivity disparity enclosed by the lithological arrays within the subsurface (Oni et al. 2017). GLSI apportions an index to each of the first-order geo-electric variables (resistivity (ρ) and thickness (h) of a layer). It is distinct from the longitudinal conductance procedure, which utilizes proportions of the first-order geo-electric variables (thickness and resistivity of layers). Given that the primary layer resistivity index rating

Publication of the European Centre for Research Training and Development -UK

is ρ_{1r} , the primary layer thickness index rating is h_{1r} , the double layer resistivity index rating is ρ_{2r} , the double layer thickness index rating is h_{2r} , the n th layer resistivity index rating is ρ_{nr} , the n th layer thickness index rating is h_{nr} and N is the number of geo-electric layers overlying the aquifer, concurring to Oni et al. (2017), GLSI can be determined utilizing the definition:

$$GLSI = \frac{\{(\rho_{1r} + h_{1r})/2 + (\rho_{2r} + h_{2r})/2 + \dots + (\rho_{nr} + h_{nr})/2\}}{N} \quad (3)$$

Tables 4 and 5 allow for the precise values of lithology-based resistivity and thickness index ratings separately. One merit of this technique is that it can be combined with GIS and remote sensing to establish an integrated method to improve the reliability of vulnerability evaluation. However, the **GLSI** technique ignores the recycling process of groundwater that contributes to the amassing of pollutants. This tendency underestimates vulnerability.

Table 4 Geo-electric layer susceptibility index (**GLSI**) rating for resistivity parameters

Resistivity range (Ωm)	Lithology	Susceptibility index rating
< 20	Clay/silt	1
20-50	Sandy clay	2
51-100	Clayey sand	3
101-150	Sand	4
151-400	Lateritic sand	2
> 400	Laterite	1

Table 5 Geo-electric layer susceptibility (**GLSI**) index rating for thickness

Thickness (m)	Index rating
< 2	4.0
2-5	3.0
5-20	2.0
>20	1.0

The designation of vulnerability index ratings based on the **GLSI** technique according to Oni et al. (2017), is summarized in Table 6.

Table 6 **GLSI** parametric rating

Index	Vulnerability rating
1.00-1.99	Low
2.00-2.99	Moderate
3.00-3.99	High
4.00	Extreme

Longitudinal conductance (S)

To a certain extent longitudinal conductance (S) is the most widely used and popularized method for aquifer vulnerability evaluation as reported in the literature (Atakpo and Ayolabi 2009; Obiora et al. 2015; Ugwu et al. 2016; Okiotor et al. 2022). According to Henriet (1976), the longitudinal conductance (S) can be utilized to ascertain the grade of protection that aquifer overlying layers offer to its fundamental groundwater contained hydrogeological units. This is often accomplished by adjusting the ratio of the layer thickness to resistivity according to Equation (4). The protective capacity rating for this method is shown in Table 7 after Oladapo and Akintorinwa (2007).

$$S = \sum_{i=1}^n \frac{h_i}{\rho_i} \quad (4)$$

Table 7 Longitudinal conductance / protective capacity rating (after Oladapo and Akintorinwa 2007).

Total longitudinal unit conductance (mhos)	Overburden classification	protective	capacity
<0.10	Poor		
0.1-0.19	Weak		
0.2-0.69	Moderate		
0.7-4.9	Good		
5-10	Very good		
>10	Excellent		

METHODOLOGY

An electrical resistivity strategy employing the VES technique was adopted in this research. The technique depicts vertical variations in apparent resistivity as a function of depth. This method is extensively utilized in alleviating hydrogeological and natural problems associated with groundwater potential and vulnerability mapping (George et al. 2014; George et al. 2017; Obiora and Ibuot 2020).

Field data were collected using the PASI-16GL conventional resistivity meter. For exploring near-surface and substantial strata, the optimum current electrode arrangement ranged from 300 to 450 m. Thirty (30) vertical electrical soundings were collected across the locale in various places. Each sounding point's GPS location was recorded in the degree, minutes and seconds (DMS) format for each instance. Figure 2 displays the procurement base map.

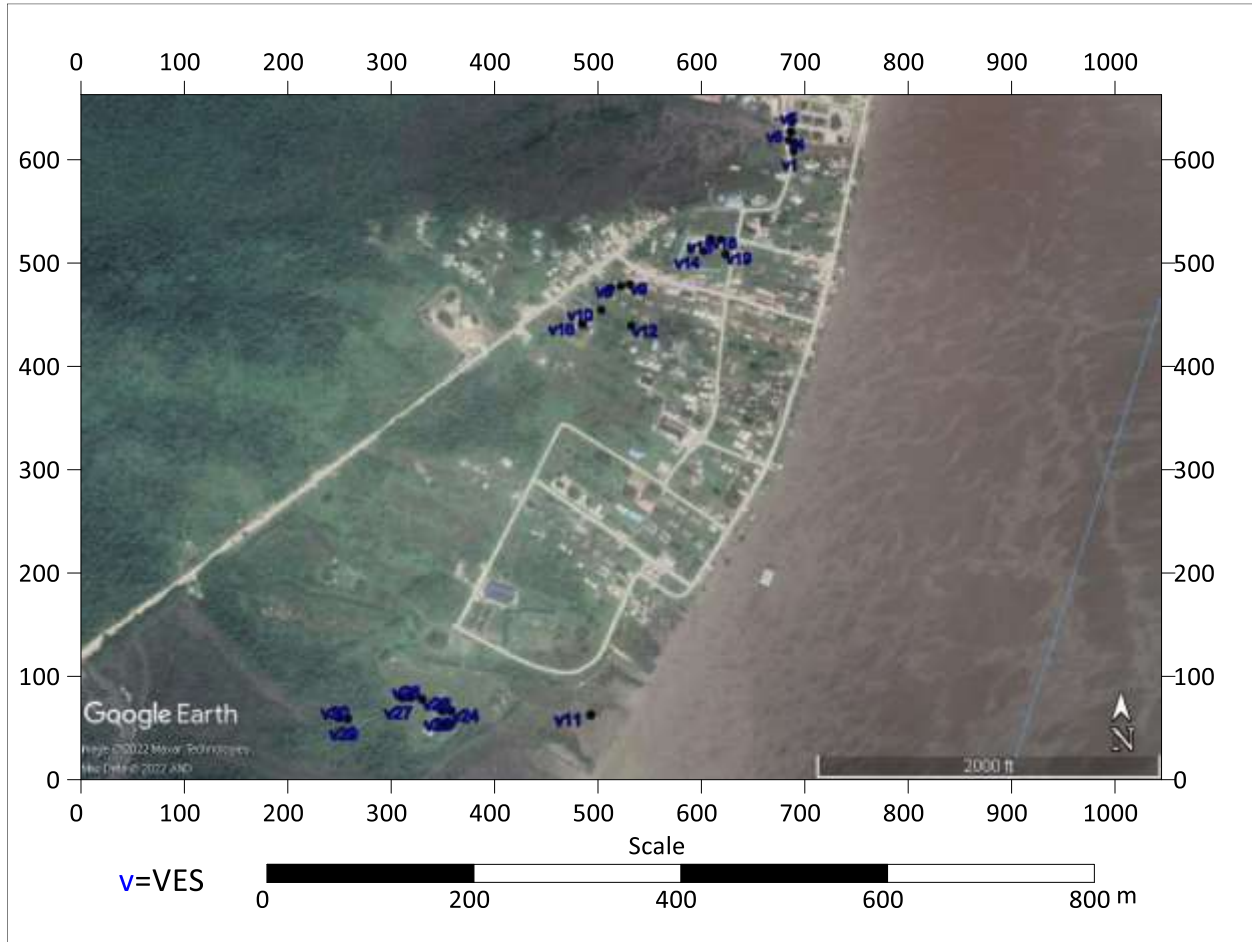


Fig. 2 Base map of data acquisition showing VES locations and physical features in the study area located at Okerenkoko community Warri Southwest, Delta State, Nigeria.

Geophysical data processing and inversion

The VES information was processed by manual curve fitting to create the resistivity demonstrate curves that were additionally curve-fitted to the auxiliary and master curves, and the layer parameters gotten were posted into the Win-Resist freeware application (Vander Velpen 2004) to get the one-dimensional resistivity models (which are thickness, depth and layer resistivity), from which the curve type for each VES point was implied from the four (4) recognized curves: **A**-curve ($\rho_1 < \rho_2 < \rho_3$), **Q**-curve ($\rho_1 > \rho_2 > \rho_3$), **K**-curve ($\rho_1 < \rho_2 > \rho_3$) and **H**-curve ($\rho_1 > \rho_2 < \rho_3$). Quantitative translation of VES information yielded the layer criteria (layer resistivity, layer thickness and depth). Layer thickness h_i , layer resistivity ρ_i and depth d_i (for the i th layer) are also known as the first-order geoelectric criteria. These first-order criteria were adapted to determine other parameters for groundwater potential assessment and vulnerability records.

Groundwater potential and vulnerability indices evaluation

In this study, a multi criteria evaluation process (MCEP) was utilized in the determination of the groundwater possibility and vulnerability indices. For groundwater possibility evaluation, the following parameters were utilized: aquifer resistivity (ρ_a), aquifer thickness (ha), coefficient of anisotropy (λ), and aquifer transmissivity (Tr).

These were mathematically defined as:

$$GW = f(\rho_a, ha, \lambda, Tr) \quad (5)$$

where, GW is groundwater, ρ_a is aquifer resistivity, ha is aquifer thickness, λ is the coefficient of anisotropy and Tr is the aquifer transmissivity.

Aquifer resistivity and thickness (water column thickness) have been consistent as criteria of hydrogeologic influence that can be utilized to appraise the groundwater possibility of an area (Rao and Briz-Kishore 1991). However, some studies have shown that coefficient of anisotropy and aquifer transmissivity are important parameters to be examined in assessing the groundwater potential of an area (Abija et al. 2019; Olorunfemi et al. 1991).

For the evaluation of the overburden coefficient of anisotropy (λ) the expression of Christensen (2000) was adopted as follows:

$$\lambda = \sqrt{\frac{\sum_{i=1}^{n-1} (h_i / \rho_i) \sum_{i=1}^{n-1} (\rho_i h_i)}{[\sum_{i=1}^{n-1} h_i]^2}} \quad (6)$$

where ρ_i and h_i are the resistivity and thickness of the layers. The coefficient of anisotropy (λ) was computed for VES 1-30. The approximate purpose of the coefficient of anisotropy is to delimit differences in the overall thickness of low resistivity materials with diverse extents of fracturing. Fracturing aids the water – retention measure in the rock, resulting in greater porosity values (Olubusola et al. 2018).

For the determination of transmissivity (Tr) we adopted the expression:

$$Tr = K \times h \quad (7)$$

Where Tr is the transmissivity in m^2/day , K is the hydraulic conductivity in m/day and h (m) is the thickness of the aquifer layer.

The hydraulic conductivity (K) was determined from geo-electric data using the expression of Heigold et al. (1979) given as:

$$K = 386.40 \rho_a^{-0.93283} \quad (8)$$

Publication of the European Centre for Research Training and Development -UK

where K is the hydraulic conductivity in m/day and ρ_a is the aquifer resistivity in Ωm . The hydraulic conductivity specifies the affluence upon which groundwater drifts over the porous rock zones. The transmissivity range and groundwater potential of an aquifer system are presented in Table 8 after Oladapo et al. (2004) as cited in Abija et al. (2019).

Table 8 Transmissivity range and Groundwater potential of aquifer system (after Oladapo et al. 2004)

TRANSMISSIVITY RANGE (m^2/day)	GROUNDWATER POTENTIAL
>500	High Potential
50.00 – 500.00	Moderate Potential
5.00 -50.00	Low Potential
0.50 – 5.00	Very low Potential
< 0.50	Negligible potential

For vulnerability index evaluation, the following indices were computed: **AVI**, **GOD-Index** and **GLSI**. Longitudinal conductance (**S**) was not computed for this study since the technique has been used to appraise the protective extent of the region in a recent study (Okitor et al. 2022).

For the computation of the aquifer vulnerability index (**AVI**), two parameters were used: the thickness (h) of the protective beds and the predicted hydraulic conductivity (K) of the protective beds. For the estimation of hydraulic conductivity (K) of the protective beds we adopted Eqn. (8) in this case ρ_a was taken as a summation of the resistivities of the protective layers protruding from the aquifer layer.

The hydraulic resistance (C) was predicted utilizing Eqn. (1). The logarithm of (C) was also computed and the vulnerability index was rated for C and $\text{Log}(C)$ as shown in Table 1.

For computation of **GOD-Index** Eqn. (2) and Table 2 were adopted, and the vulnerability index was rated using Table 3.

For computation of the geo-electric layer susceptibility index (**GLSI**), Eqn. (3) and Tables 4 and 5 were adopted, and the vulnerability index was rated using Table 6.

RESULTS AND DISCUSSIONS

Groundwater potential evaluation

Table 9 summarizes the results of VES interpretation, showing the aquifer resistivity, aquifer thickness, hydraulic conductivity, transmissivity and coefficient of anisotropy for VES 1-30. The curve categories consist of H, K and Q curves, with K and Q being predominant (Table 9). The aquifer resistivity and thickness for VES 1-30 are indicated in Table 9. Contour maps of aquifer resistivity, aquifer thickness, hydraulic conductivity, transmissivity and coefficient of anisotropy were utilized to evaluate the groundwater possibility of the study area.

The aquifer layer resistivity map of the study area (**Fig. 3**) depicts the alteration of resistivity in the aquifer layers at the study area. The aquifer resistivity outline demonstrates that the area is defined by three plausible groundwater sections: low, moderate and high established on their resistivity values. Essentially, resistivity in sedimentary rocks is determined by drained space, extent of sorting and grain content distribution (Reynolds 1997; Archie 1942). Thus, within an aquifer, groundwater discharges from higher resistivity sections (with little porosity) to minor resistivity sections (with large porosity). This gives a hint that, enclosed by the aquifer, sections that are less resistive favor saturation as a result of high porosity and possess a high groundwater potential (GPZ). In **Fig. 3**, aquifers with relatively low resistivity values are found in VES 1, 3, 6, 7, 8, 11, 13, 15, 16, 17, 18, 19, 20, 21, 24, 25, 26, 27, 28, 29 and 30 of the investigated areas while moderate and high values are found in VES 2, 4, 5, 9, 10, 12, 14, 22 and 23 locations of the study area.

Table 9 Summary of VES Interpretation showing the model resistivity parameters (layer resistivity and thickness), curve types, and estimated hydraulic conductivity, transmissivity and coefficient of anisotropy values

VES Stn.	Layer resistivity ($\rho_1/\rho_2/\rho_3/\dots/\rho_n$)	Curve type	Layer thickness ($h_1/h_2/h_3/\dots/h_n$)	$\sum \rho_{(n-1)}$ (n = aquifer layer)	$\sum h_{(n-1)}$ (n = aquifer layer)	Hydraulic conductivity K_i (m/day)	Tr $T_r = K_x h_a$ (m^2/day)	COA (λ)
VES 1	102.6/93.9/24.5/4.5/1.6/225.0*	Q-Q-Q-H	0.6/2.3/7.4/23.2/31.3/33.5*	227.1	64.8	2.4496	82.061 6	4.61042 9
VES 2	67.9/49.5/6.7/1.5/340.1*	Q-Q-H	0.7/3.3/12.5/62.5/37.7*	125.6	79.0	4.2563	160.46 25	6.51214 3
VES 3	266.2/36.2/92.3/5.7/2.3/337.0*	H-K-Q-H	0.5/2.3/2.8/20.8/22.1/26.4*	402.7	48.5	1.4356	37.899 8	4.77951 4
VES 4	41.2/20.0/78.5/7.2/1.4/226.0*	H-K-Q-H	0.4/2.1/1.7/24.9/39.9/29.2*	148.3	69.0	3.6453	106.44 28	4.84551 6
VES 5	388.8/58.7/14.8/5.6/270.7*	Q-Q-H	0.7/3.2/8.3/47.0/12.0*	467.9	59.2	1.2481	14.977 2	2.70423 9
VES 6	64.5/30.2/213.8/15.0/230.0*	H-K-H	0.5/1.6/2.4/29.5/2.4*	94.7	2.1	5.5391	13.293 8	1.56721
VES 7	96.0/169.1/23.7/8.4/151.4*	K-Q-H	0.6/3.3/17.7/15.8/21.5*	297.2	37.4	1.9059	40.976 9	1.88788 1
VES 8	202.8/349.6/61.8/14.2/205.5*	K-Q-H	0.7/1.9/8.3/30.0/25.1*	628.4	40.9	0.9479	23.792 3	1.94127 7
VES 9	316.6/511.1/64.1/14.5/190.0*	K-Q-H	0.6/1.3/6.5/12.8/19.3*	906.3	21.2	0.6736	13.000 5	1.84537

Publication of the European Centre for Research Training and Development -UK

VES 10	92.1/124.6/24.9/80 0.0*	K-H	0.7/4.0/48.2/10. 1*	241.6	52.9	2.3121	23.352 2	2.22044 6
VES 11	164.8/295.4/31.0/7 .9/443.0*	K-Q- H	0.7/1.9/2.6/26.2 /13.7*	499.1	31.4	1.1751	16.098 9	3.44988 1
VES 12	469.3/1190.2/145. 8*	K-Q	0.9/2.6/6.1/6.1*	1659.5	3.5	0.3831	2.3369	2.70767 7
VES 13	605.2/881.2/189.7 *	K-Q	0.8/2.4/8.2*	1486.4	3.2	0.4246	3.4817	1.22930 3
VES 14	670.2/649.9/842.0 *	H-K	0.7/4.4/7.4*	1320.1	5.1	0.4743	3.5098	1.00787 2
VES 15	738.1/820.8/314.2 *	K-Q	0.7/2.3/7.2*	1558.9	3.0	0.4061	2.9239	1.09366 7
VES 16	618.0/1594.4/206. 9*	K-Q	0.8/2.2/8.9*	2212.4	3.0	0.2930	2.6077	1.37309 7
VES 17	642.2/1518.6/121. 8*	K-Q	0.8/2.6/7.4*	2160.8	3.4	0.2995	2.2163	1.71164
VES 18	790.6/1162.1/197. 3*	K-Q	1.0/2.6/6.8*	1952.7	3.6	0.3292	2.2386	1.34503
VES 19	635.6/1435.4/252. 8*	K-Q	0.7/2.4/7.2*	2071.0	3.1	0.3116	2.2435	1.29699 3
VES 20	443.7/1078.3/199. 6*	K-Q	1.1/3.5/21.2*	1522.0	4.6	0.4153	8.8044	1.19512 9
VES 21	1150.3/961.2/170. 9*/24.1	Q-Q- H	0.7/4.8/14.2*/39 .7	2111.5	5.5	0.3060	4.3452	2.08109 2
VES 22	1867.5/467.8/63.8/ 227.3*	Q-H	1.3/9.1/61.1/22. 1*	2399.1	71.5	0.2717	6.0046	1.38385
VES 23	645.7/864.0/148.9 *	K-Q	0.8/3.4/23.6*	1509.7	4.2	0.4185	9.8766	1.21478 6
VES 24	266.4/760.7/138.5/ 16.5/140.6*	K-Q- H	0.8/3.2/14.8/48. 6/42.4*	1182.1	67.4	0.5257	22.192 2	1.78747 3
VES 25	230.8/817.4/118.4/ 21.2/448.4*	K-Q- H	0.9/3.4/4.8/19.8 /23.4*	1187.8	28.9	0.5234	12.247 6	2.33944 3
VES 26	86.9/214.6/18.2/19 6.4*	K-H	0.8/5.9/24.8/14. 2*	319.7	31.5	1.7805	25.283 1	1.79565 3
VES 27	61.3/250.2/103.0*	K-Q	1.0/3.9/9.2*	311.5	4.9	1.8242	16.782 6	1.10005 7
VES 28	13.8/43.0/262.8*	A	1.0/5.1/2.1*	56.8	6.1	8.9234	18.739 1	1.52442 7
VES 29	162.7/631.4/298.7/ 29.4/118.8*	K-Q- H	0.9/3.2/6.7/49.1 /26.7*	1122.2	59.9	0.5519	14.735 7	1.50264 7

VES 30	951.4/2258.5/200.	K-Q-	0.8/2.5/13.0/53.	3438.3	69.3	0.1942	7.1077	1.74085
	8/27.6/117.8*	H	0/36.6*					5

*Aquifer layer resistivity; *Aquifer layer thickness

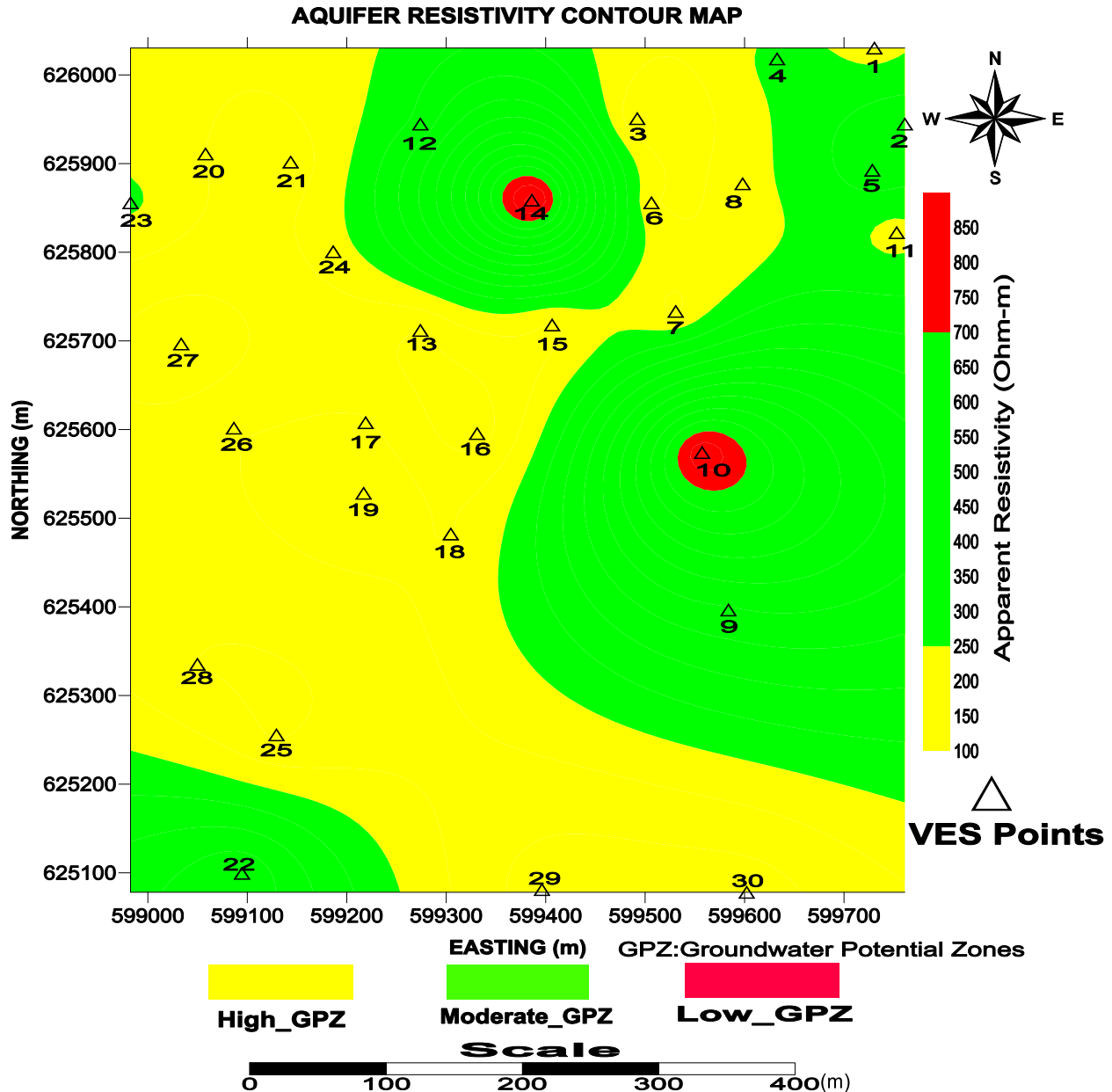


Fig. 3 Aquifer resistivity contour map of the study area

The aquifer thickness contour outline is laid out in Fig. 4. The aquifer layer thickness (Fig. 4) ranges from 2.0 to 42.0 m. Sections amidst thicknesses of 2.0 – 8.0 m are expressed as low and

these areas are found in VES 10, 12, 14, 15, 16, 17, 18, 19, 23, and 27 (Fig. 4). Sections of aquifer thicknesses between 10.0 and 32.0 m; 34.0 and 42.0 m are considered moderate and high respectively and these areas are found in VES 1, 2, 3, 4, 5, 6, 7, 8, 9, 11, 13, 20, 21, 22, 24, 25, 26, 28, 29 and 30 of the investigated area.

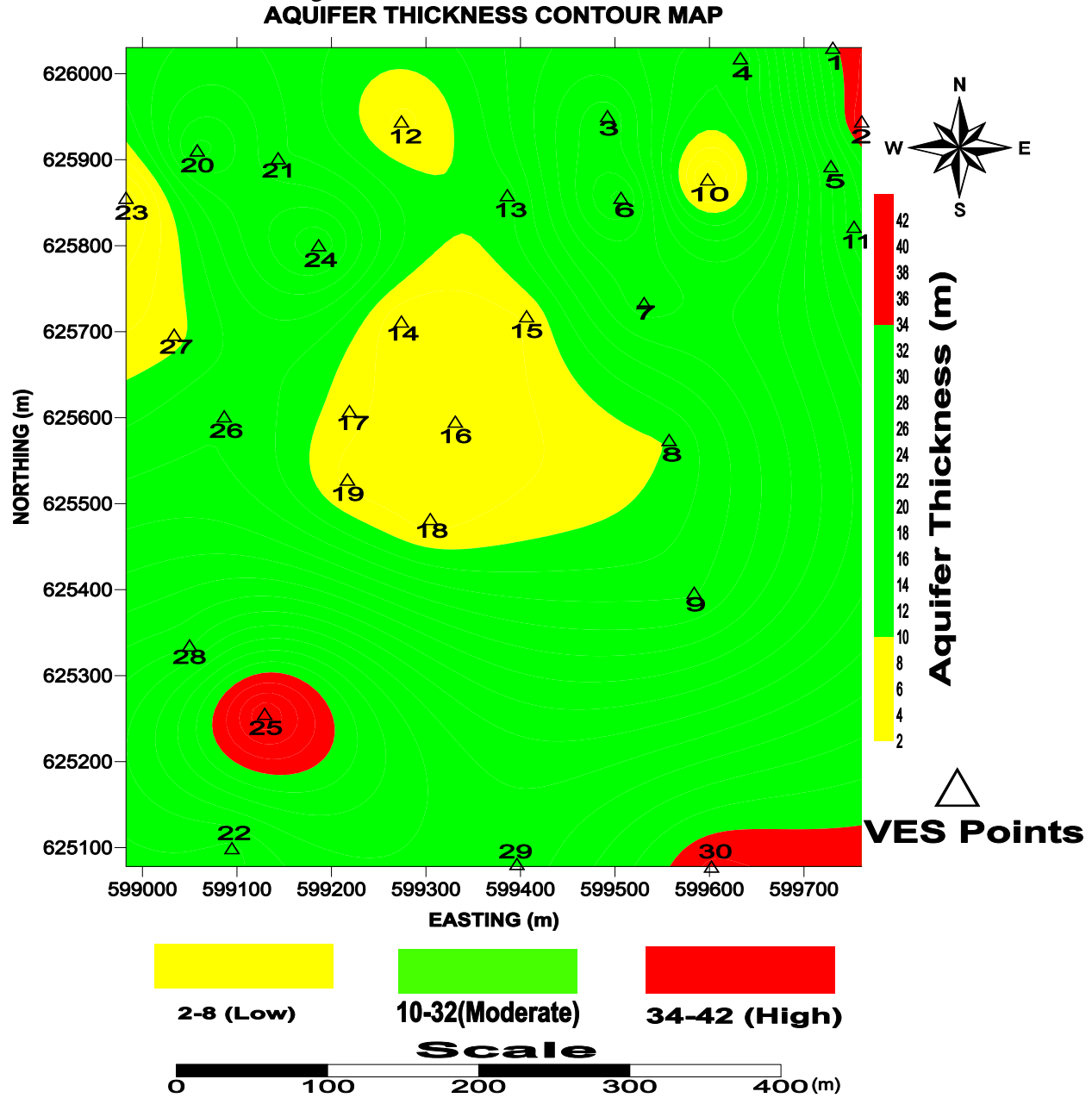


Fig. 4 Aquifer thickness contour map of the study area

The hydraulic conductivity outline of the study area (**Fig. 5**) displays the divergence of hydraulic conductivity among the aquifer layers identified from VES 1 to 30. The hydraulic conductivity extends from 0.1942-8.9234 m/day (Table 9). These values were used in computing the transmissivity potential of the area which was further used in rating the groundwater possibility of the area. The transmissivity potential contour map is shown in **Fig. 6**. The map was segmented into three colors (blue, red and yellow). The blue color represents areas with moderate groundwater potential; the predominant red color represents areas with minor groundwater possibility; and at the same time the yellow color represents areas with very low groundwater potential (Tables 8 and 9). The transmissivity map shows that the groundwater prospect of the area is predominantly little as most of the VES points were categorized under the red and yellow colors (**Fig. 6**). The coefficient of anisotropy contour map is shown in **Fig. 7**. The approximate utility of this parameter is to alternate changes in the overall thickness of low resistivity aquifer formations. The estimated values of coefficient of anisotropy range from 1.007872 to 6.512143 (Table 9), which delineates the actual alteration of the anisotropy attribute of rock formations. The regions with high magnitudes of coefficient of anisotropy (VES 2) propose that the fracture framework in this area must have stretched in all directions inside the rock, ensuing in greater porosity. Additionally, zones that show low values of coefficient of anisotropy show unidirectional stretch in fracture. Consequently, such zones may not deliver good supply of water.

From the multi-criteria assessment carried out in this study, it was realized that the present geoelectric structures in VES 1, 2 and 4 have shown consistency in their groundwater potential and yield within these zones judging from their aquifer resistivity, thickness, transmissivity and coefficient of anisotropy values. From the aquifer resistivity outline (**Fig. 3**), VES 1 showed high groundwater potential, while VES 2 and 4 showed moderate groundwater potential respectively. From aquifer thickness values (**Fig. 4**), VES 1 and 4 showed moderate thickness respectively, while VES 2 showed high thickness. From transmissivity potential values (**Fig. 6**), VES 1, 2 and 4 showed moderate groundwater potential respectively, while coefficient of anisotropy values (**Fig. 7**), for VES 1, 2 and 4, showed moderate values for VES 1 and 4, respectively and a high value for VES 2.

Vulnerability Indices evaluation

The vulnerability indices (**AVI**, **GOD** and **GLSI**) and their respective ratings are briefed in Table 10. The vulnerability index amounts in Table 10 were used to generate vulnerability index maps using terrain and 3-D surface modeling application (Surfer 2002), employing the advanced contour level category. In this contouring option, the contour lines are hidden and exchange for representative colors utilized to spread the protection capacities for each vulnerability index, as shown in Table 10.

Figures 8 a and b are the aquifer vulnerability index (**AVI**) maps for (**C**) and $\log(C)$ respectively (**C** is the hydraulic resistance). Hydraulic resistance is a vital aquifer specification that is employed in gauging the opposition of an aquifer to vertical leakage of fluid through its shielding layers, and

the correlation bounded by the aquifer vulnerability index (**AVI**) and C and $\log C$ is shown in Table 1. The **AVI-C** map (**Fig. 8a**) displays that the AVI rating in the majority of the VES-locations was ranked high to extremely high (yellow and red colors), and this indicates that aquifers in these locations are vulnerable to pollution, while VES 24, 25, 29 and 30 were rated moderate (in the blue color). The **AVI-log C** map (**Fig. 8b**) which is the logarithmic/filtered equivalent of **AVI-C** (**Fig. 8a**) was also contoured with the SURFER-13 program. In **Fig. 8b**, it was observed that most of the VES-locations that ranked extremely high vulnerability index (red color in **Fig. 8a**) have been filtered to high vulnerability index (VES 3, 11, 13, 16, 17, 18 and 26), while VES 24, 25, 29 and 30 which ranked moderate (blue color in **Fig. 8a**), have been filtered to retain only VES 24 and 30 in this category (blue color in **Fig. 8b**). This observation validates the assertion that the logarithm operator is a filter that attenuates numeric variables to give more refined values.

The **GOD**-Index (groundwater occurrence (**G**), lithology of the overlying aquifer (**O**), and depth to the aquifer (**D**)) values in Table 10 were contoured to produce the **GOD** map laid out in **Fig. 9**. The **GOD** outline depicts that the vulnerability index rating in the study area is ranked negligible (0.0-0.1), low (0.1-0.3) and moderate (0.3-0.5) with most of the VES-locations (VES 3, 6, 7, 9, 12, 13, 14, 15, 16, 17, 18, 19, 20, 21, 23 and 28) ranked low to moderate (red and blue colors), which indicates that these locations are susceptible to vulnerability.

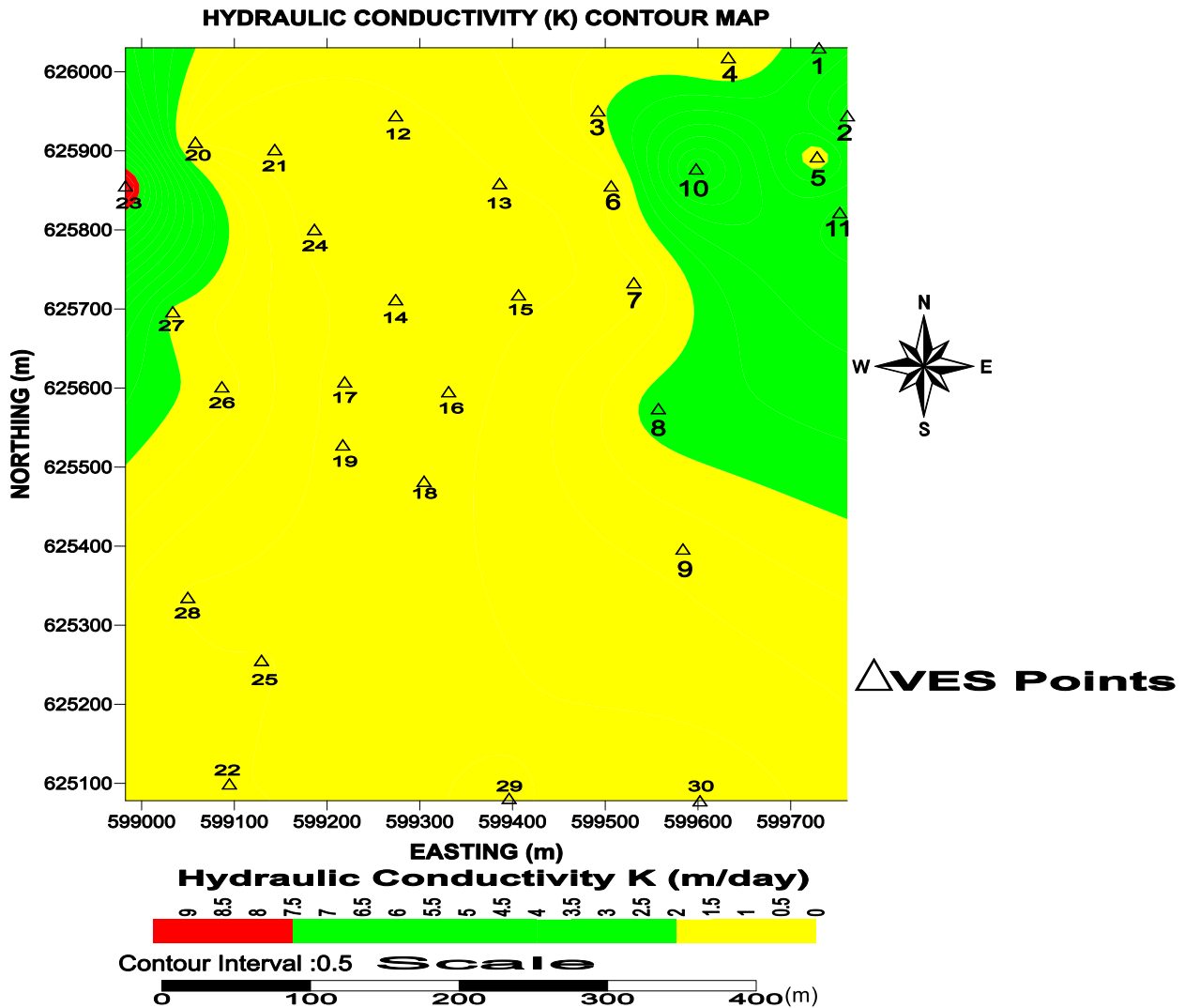


Fig. 5 Hydraulic conductivity contour map of the study area

The **GOD**-Index outline was fitted in distinction to the layers overlying the aquifer and it incorporates the response of noticeable layer **GOD** parameters. The **GOD** outline in Fig. 9 identifies the divergence of the groundwater vulnerability to defilement within the study area.

The **GLSI** values in Table 10 were also contoured to produce the **GLSI** map shown in Fig. 10. The **GLSI** map in Fig. 10 was fitted from the outcome of lithology and layer thickness in the aquifer vulnerability evaluation because amply massive beds overlying the aquifer can retard the travel pace of pollutants into the aquifer layer, thereby, minimizing the response of pollutants in aquifers. The **GLSI** map in Fig. 10 shows that the vulnerability index rating in the study area is ranked moderate (2.00-2.99), high (3.00-3.99) and extremely high (≥ 4.00), with most of the VES-locations ranked moderate to high (blue and yellow colors), with exception of VES 27, which

ranked extremely high (red color). This result pinpoints that the region is prone to vulnerability with a diversity ranging from moderate, high to extremely high vulnerability as marked in Table 10.

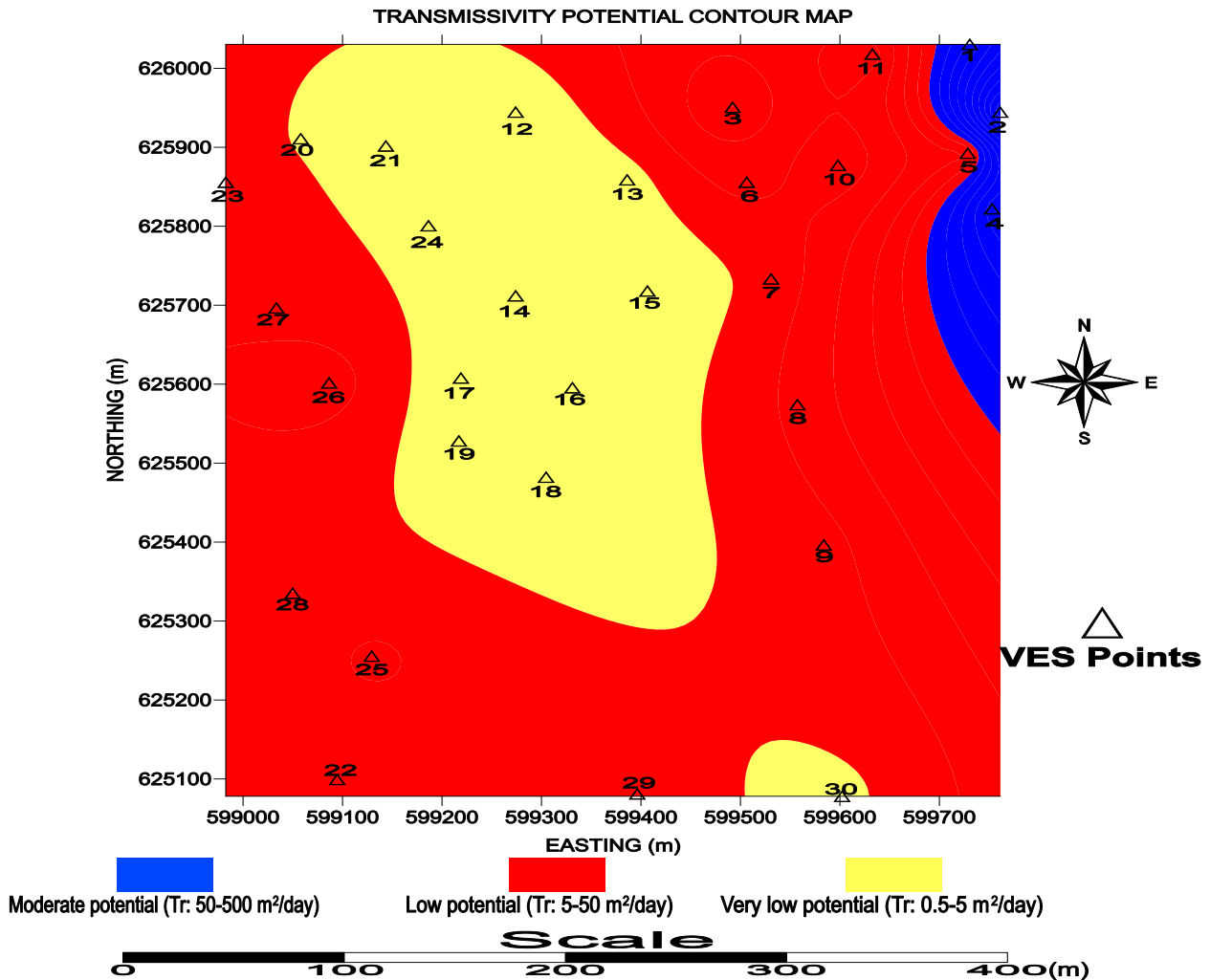


Fig. 6 Transmissivity potential contour map of the study area

The multi-criteria evaluation using hydrogeophysical criteria in sync with index-based methods facilitated the evaluation of **AVI**, **GOD** and **GLSI** models for aquifer vulnerability assessment. By relating the **AVI**, **GOD** and **GLSI** results in Table 10, some VES-locations showed convergence in their vulnerability index rating established from the hydrogeological and index-based perspectives. VES 8 and 10 showed high vulnerability indices adjudged from their **AVI** and **GLSI** models, VES 12, 13, 14, 15, 16, 17, 18, 19 and 20 showed extremely high to high, moderate and high vulnerability indices adjudged from their **AVI**, **GOD** and **GLSI** models; and VES 22, 24, 29 and 30 scored negligible to moderate vulnerability indices from their **GOD**, **AVI**, and **GLSI** models. VES 23 and 28 scored extremely high to high vulnerability from the **AVI** and **GLSI**

models, while VES 27 scored extremely high in both the AVI and GLSI indices. These findings validate the adoption of a multi-criteria evaluation methodology in aquifer vulnerability studies. The vulnerability marks of each of the models facilitated the likelihood of building the vulnerability index maps shown in Figs. 8, 9 and 10. The maps altogether indicate different scores of susceptibility of the aquifer to defilement with a band of disparities that are not remarkably far from the scope of poor protective measures in the region. The vulnerability maps guide decision-making logistics regarding monitoring and conservation of groundwater quality.

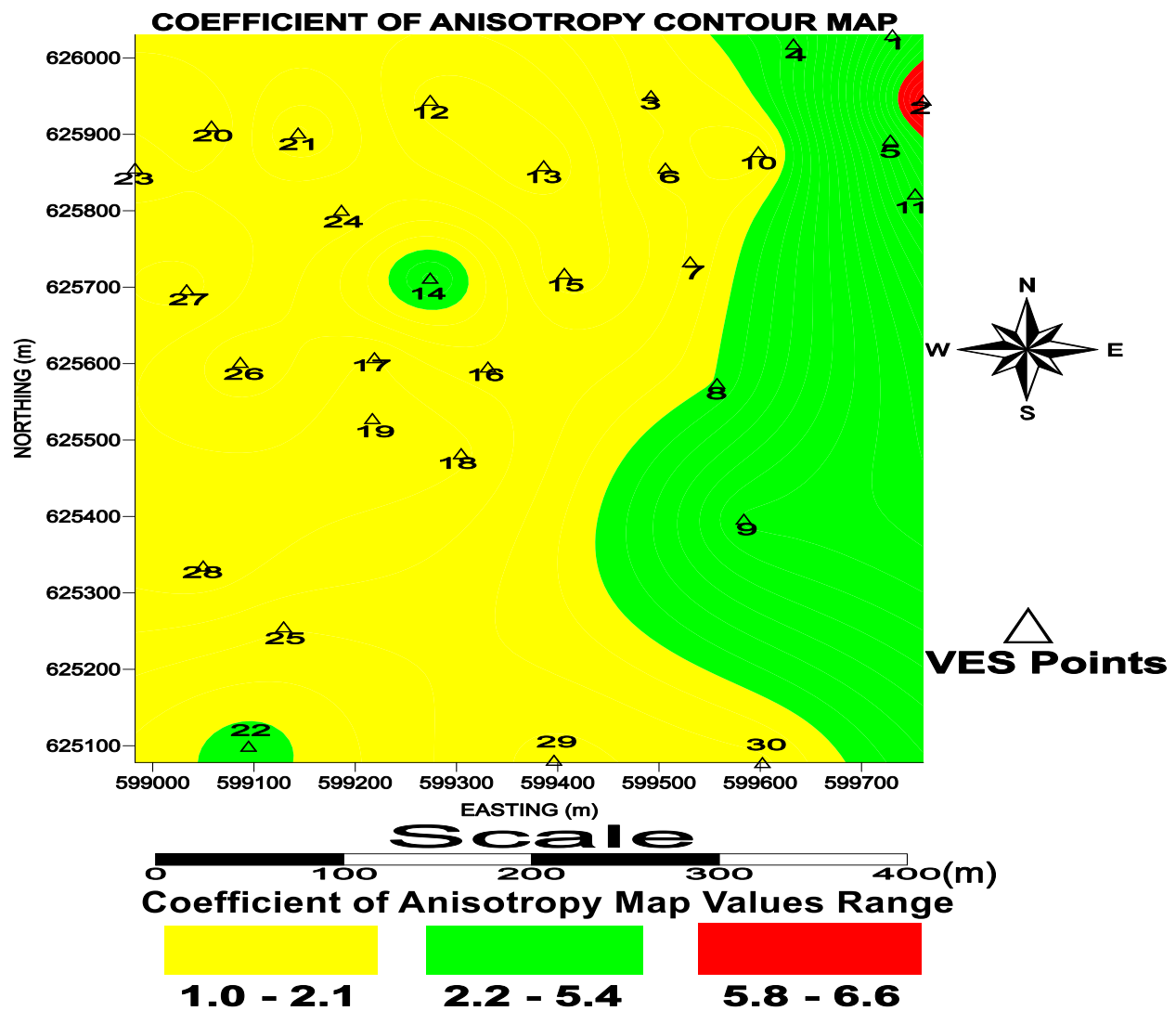
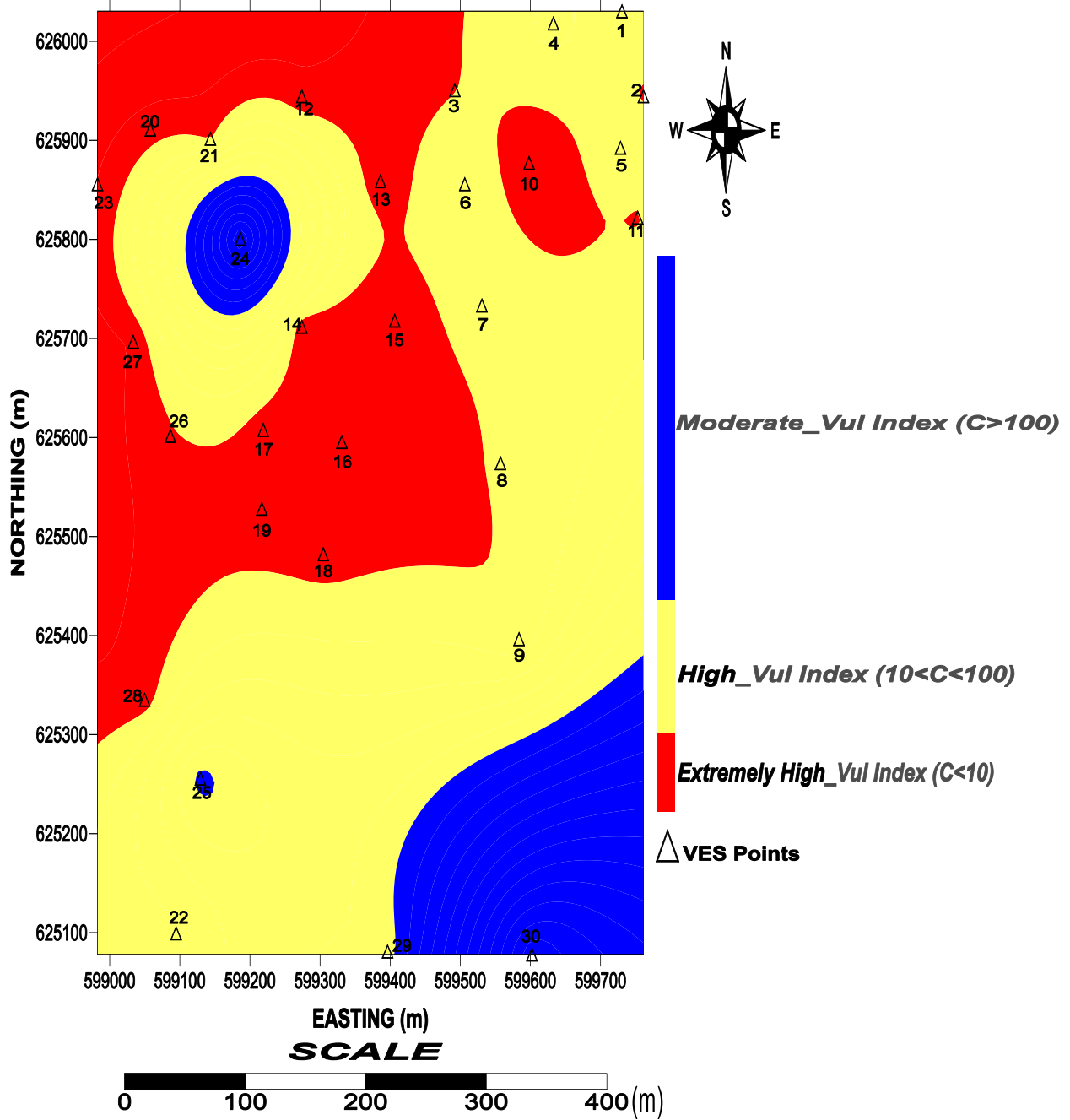


Fig. 7 Coefficient of anisotropy contour map of the study area

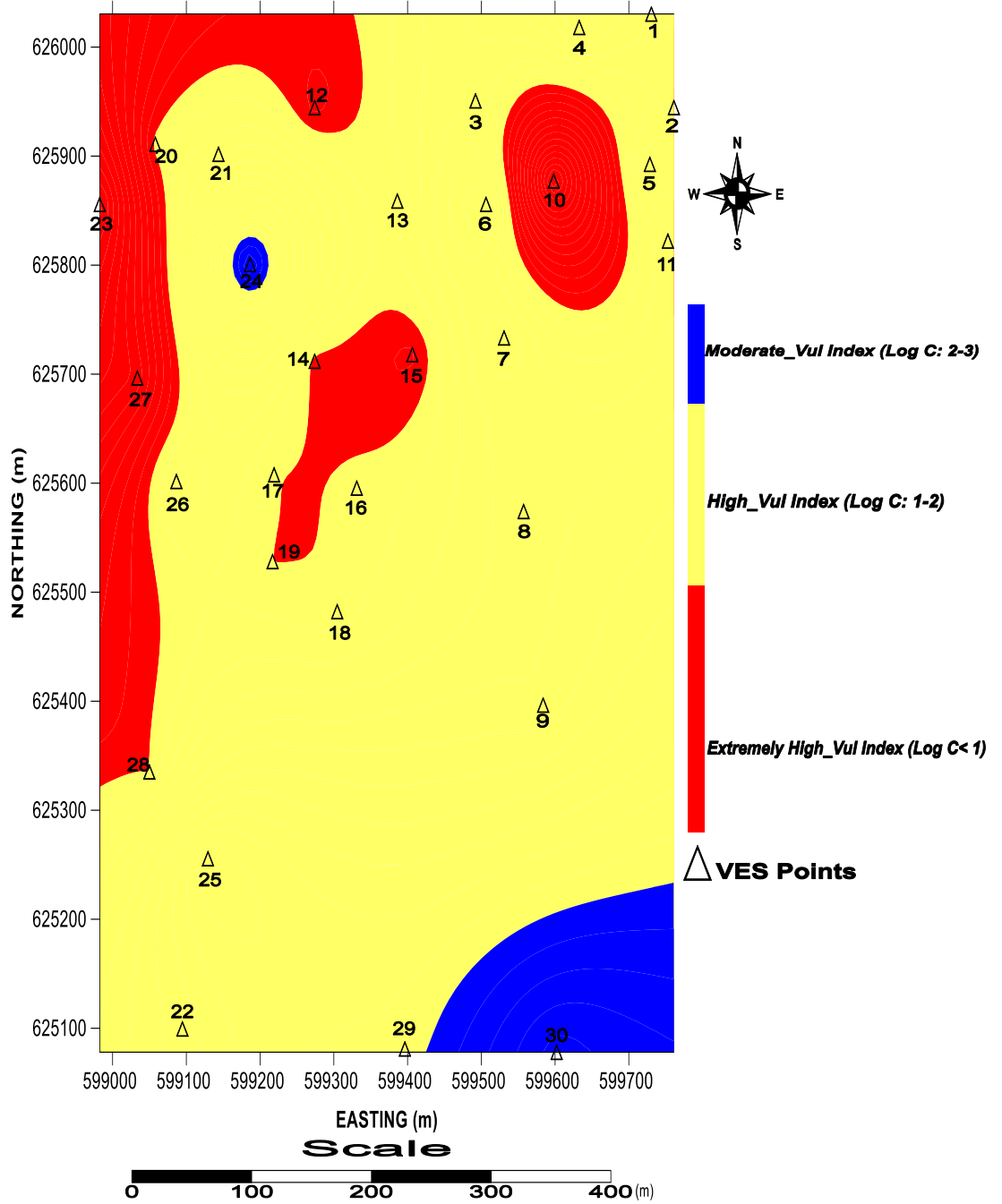
AQUIFER VULNERABILITY INDEX (AVI) MAP FROM HYDRAULIC RESISTANCE (C)



(a) AVI contour map from hydraulic resistance (C)

(b)

AQUIFER VULNERABILITY INDEX (AVI) MAP FROM LOGARITHM OF HYDRAULIC RESISTANCE (Log C)



(d) AVI contour map from Log C

Fig. 8 Aquifer Vulnerability Index (AVI) contour map (a) From hydraulic resistance (C) (b) From logarithm of C

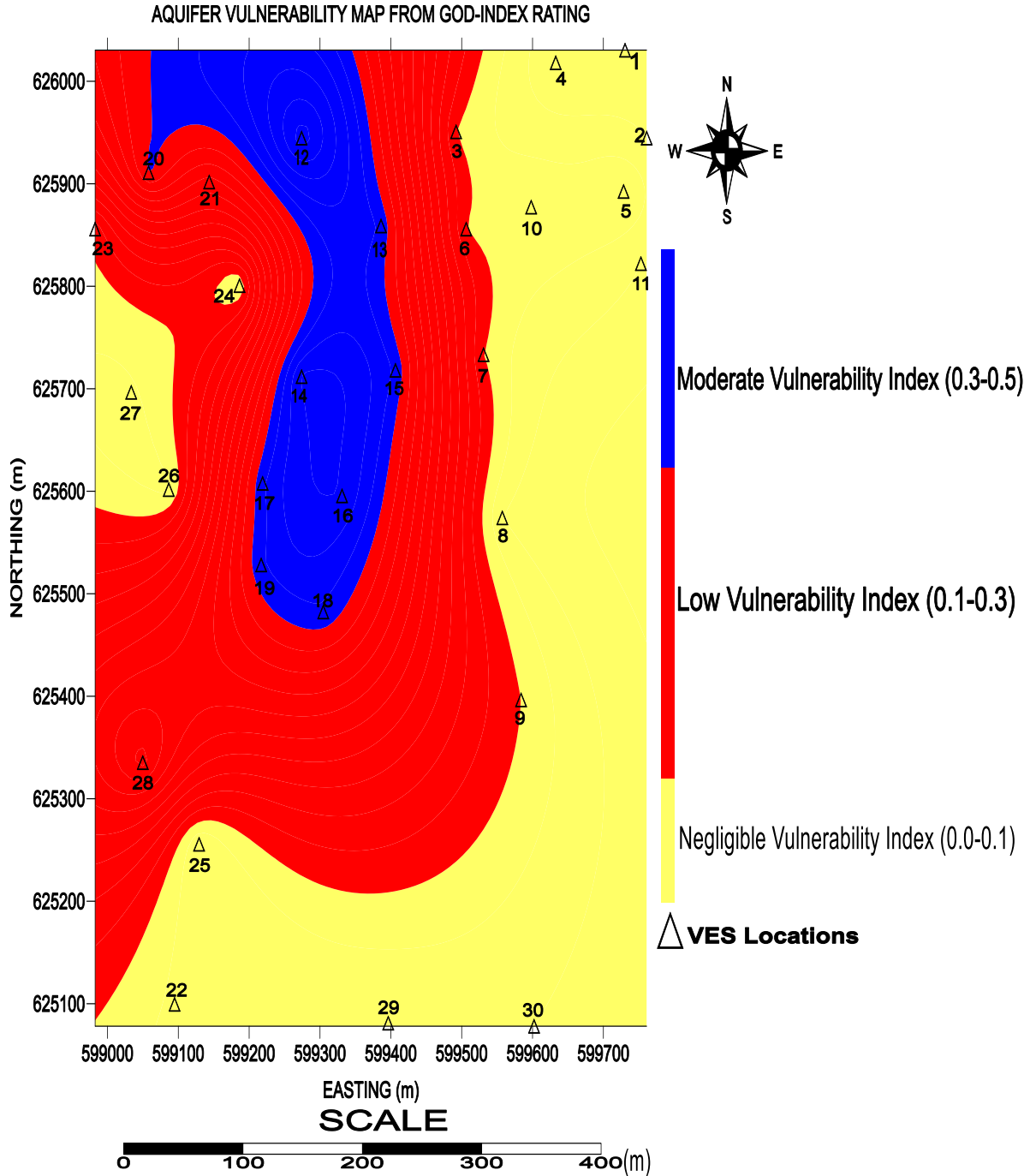


Fig. 9 GOD-Index contour map

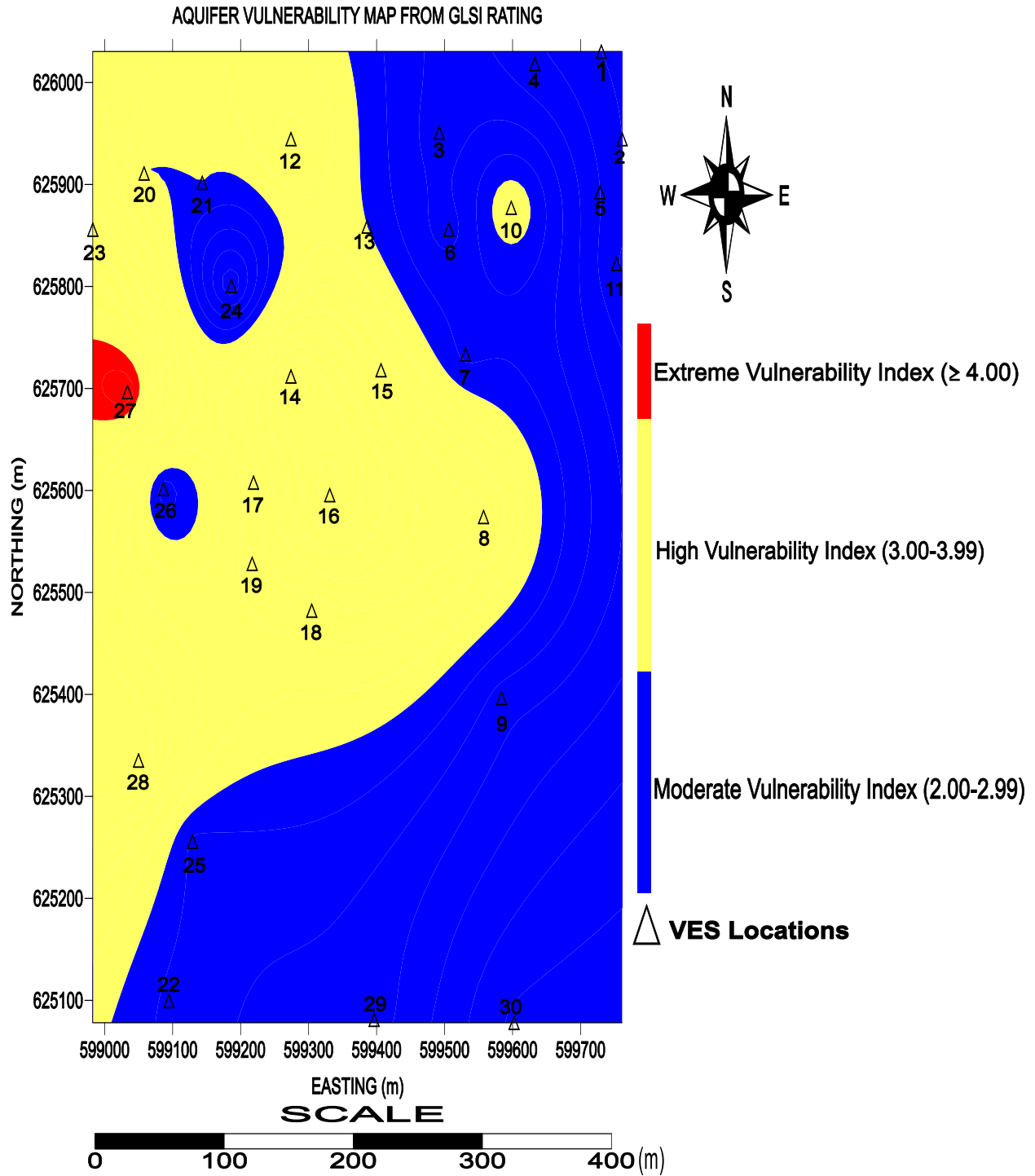


Fig. 10 GLSI contour map

Table 10 Summary of computed Vulnerability indices and ratings in the study area

VES Stn.	C (Years)	Log (C) = AVI	AVI Rating	GOD Index	GOD Index Rating	GLSI	GLSI Rating
VES 1	26.4538	1.4225	High	0.06	Negligible	2.50	Moderate
VES 2	18.5607	1.2686	High	0.08	Negligible	2.50	Moderate
VES 3	33.7839	1.5287	High	0.12	Low	2.60	Moderate
VES 4	18.9286	1.2771	High	0.08	Negligible	2.50	Moderate
VES 5	47.4333	1.6761	High	0.06	Negligible	2.625	Moderate
VES 6	10.379	1.0162	High	0.12	Low	2.90	Moderate
VES 7	19.6231	1.2928	High	0.12	Low	2.75	Moderate
VES 8	43.1484	1.6350	High	0.100	Negligible	3.00	High
VES 9	31.4725	1.4979	High	0.12	Low	2.87	Moderate
VES 10	2.8793	0.4593	High	0.08	Negligible	3.33	High
VES 11	6.7204	1.4268	High	0.098	Negligible	2.75	Moderate
VES 12	9.1353	0.9607	Ext. High	0.384	Moderate	3.75	High
VES 13	7.5366	1.1772	Ext. High	0.336	Moderate	3.25	High
VES 14	10.7530	1.0315	High	0.336	Moderate	3.00	High
VES 15	7.3865	0.8684	Ext. High	0.432	Moderate	3.25	High
VES 16	9.984	1.0103	High	0.336	Moderate	3.25	High
VES 17	9.399	1.0551	High	0.378	Moderate	3.75	High
VES 18	10.009	1.0389	High	0.336	Moderate	3.25	High

Publication of the European Centre for Research Training and Development -UK

VES 19	9.9485	0.9978	Ext. High	0.336	Moderate	3.25	High
VES 20	10.0757	1.0444	High	0.324	Moderate	3.00	High
VES 21	17.9723	1.2546	High	0.252	Low	2.999	Moderate
VES 22	26.1961	1.9203	Moderate	0.100	Negligible	2.50	Moderate
VES 23	10.0364	0.9016	Ext. High	0.288	Low	3.50	High
VES 24	128.1996	2.1079	Moderate	0.08	Negligible	2.875	Moderate
VES 25	155.2171	2.0000	High	0.096	Negligible	2.875	Moderate
VES 26	17.6918	1.2478	High	0.096	Negligible	2.833	Moderate
VES 27	2.6862	0.4291	Ext. High	0.098	Negligible	4.00	Extreme
VES 28	0.6836	-	Ext. High	0.128	Low	3.50	High
VES 29	108.5392	1.0356	Moderate	0.08	Negligible	2.75	Moderate
VES 30	356.8648	2.5525	Moderate	0.08	Negligible	2.375	Moderate

CONCLUSIONS

Ground-acquired electrical resistivity data consisting of thirty (30) Schlumberger-VES were obtained in Okerenkoko community in Warri-Southwest, Delta State, to assess the groundwater potential and vulnerability indices of the area by means of a multi-criteria evaluation methodology. The VES data was used to obtain the first-order geoelectric variables, which were further exploited in calculating the geo-hydraulic parameters of the aquifer (hydraulic conductivity and transmissivity) and vulnerability indices (**AVI**, **GOD**, and **GLSI**) for an aquifer vulnerability appraisal of the area. The groundwater prospect of the area was graded based on the aquifer resistivity, thickness, transmissivity and coefficient of anisotropy values of the aquifer layers defined for VES 1-30. The results show that aquifer layers with low resistivity tend to be more saturated as a result to their immense porosity, thus displaying a higher groundwater potential compared to aquifer layers with high resistivity. The geoelectric structures defined in VES 1, 2 and 4 were consistent in their groundwater potential and yield judging from the multi-criteria evaluation employed (aquifer resistivity, thickness, transmissivity and coefficient of anisotropy

values). The multi-criteria evaluation of vulnerability indices using hydrogeophysical parameters and index-based methods facilitated the computation of **AVI**, **GOD** and **GLSI** models for aquifer vulnerability assessment. The models depend on the symbiotic effects of geologic array and thickness as the basis for the magnitude of conservation imparted to any particular aquifer involved. The **AVI** model shows that most of the VES-locations were rated high to extremely high in their vulnerability and indicates that aquifers in these locations are vulnerable to pollution. The extent of vulnerability was amplified by the **AVI** model more than the **GOD** and **GLSI** models because the **AVI** model accords higher priority to the geologic lithological thickness than the essential characteristics of the geologic layers. The extent of vulnerability in the **GOD** model was below the **AVI** model because the **GOD** model accords greater inclination to inherent characteristics of geologic entities on the grounds of a geologic unit's grain size distribution, extent of compaction, consolidation and other implicit descriptions that alter the hydrogeophysical and geo-electrical structure of a geologic bed. The study also showed that the **GLSI** model, because of each individual's conjunction support for superimposed layer thicknesses, is a useful method for identifying hydrogeological entities that are affected by pollution. Aquifer-superimposed layers that are excessively thick may slow down the rate at which pollutants enter the aquifers underneath. The comparable zone is only somewhat susceptible to pollution from linked toxins as a result of this process, which delays and reduces contaminants resulting from the symbiotic fallout of geology and biogenic activities. By correlating the results of vulnerability index maps for the **AVI**, **GOD**, and **GLSI** models for the VES-locations, more correlation was observed for the **AVI** and **GLSI** models. These findings validate the adoption of a multi-criteria evaluation methodology for aquifer vulnerability studies and are stoutly recommended for possible groundwater development planning and management.

Acknowledgement

The authors profoundly acknowledge the good people of the Okerenkoko community for allowing us to carry out the geophysical survey used for this study within the community and the Federal University of Petroleum Resources, Effurun, Nigeria, for the use of their computing facilities. We are also indebted to Dr. N.J. George (Associate Professor) at the Department of Physics, Akwa Ibom State University, Nigeria, for guiding us in the index-model computation.

Declarations

Ethical approval, consent to participate and consent to publish N/A.

Funding

There was no grant or financial support provided from any agency in the public, commercial and not-for profit organization for this research work.

Code availability (Software used)

Arc-GIS, Microsoft Excel, Sufer-13 and Winresist-Suite.

Competing Interests

We declare that this research work has never been submitted previously by anyone to any journal for peer review and publication; hence it is an original work. The authors declare no competing interests.

REFERENCES

- Abija FA (2018) Gap analysis and strategic implementation of environmental impact assessment a pathway to achieving the SDGs in Nigeria. *International Journal of Environmental Monitoring and Protection*, 5(4): 81-86.
- Abija FA, Nse UE, Abam TKS, Abimbola II (2019) Assessment of Aquifer Hydraulic Properties, Groundwater Potential and Vulnerability Integrating using Geoelectric Methods with SRTM -DEM and LANDSAT-7 ETM lineament Analysis in Parts of Cross River State, Nigeria, *London J. of Research in Science*: 19(7), 35-51.
- Adiat AN, Nawawi MNM, Abdullah K (2013) Application of Multi-Criteria Decision Analysis to Geo-electric and Geology Parameters for Spatial Prediction of Groundwater Resources Potential and Aquifer Evaluation”, *Pure Appl. Geophys*, 170(3), 170, 453–471 ISSN 0033 4553.
- Agoubi B, Dabbaghi R, Kharroubi A (2018) A Mamdani adaptive neural fuzzy inference system for improvement of groundwater vulnerability. *Groundwater* 56(6):978–985. <https://doi.org/10.1111/gwat.12634>.
- Amaize E (2006) Oil spill in Olomoro destroys aquatic life and economic crops. *Vanguard Newspaper*, 13th September: 20.
- Archie GE (1942) The electrical resistivity log as an aid to determining some reservoir characteristics. *Trans AIME* 146(1):389–40
- Assez OL (1989) Review of the stratigraphy, sedimentation and structure of the Niger Delta. In: Kogbe (ed) *Geology of Nigeria*, Rock View (Nig.) Ltd., Jos, pp 311–324.
- Atakpo EA, Ayolabi EA (2009) Evaluation of aquifer vulnerability and the protective capacity in some oil producing communities of western Niger Delta. *Environmentalist* (29): 310–317. DOI:10.1007/s10669-008-9191-3
- Chernicoff AE, Whitney IK (2009) *An introduction to physical planning*; Houghton Mifflin Company, New York.
- Christensen NB (2000) Difficulties in determining Electrical Anisotropy in Subsurface Investigations: *Geophysical Prospecting (EAGE)*, 48(1): 1-19.
- Doust H, Omatsola E (1990) Niger-Delta. In: Edwards, J.D. and Santogrossi, P.A., Eds., *Divergent/Passive Margin Basins*, AAPG Memoir 48, American Association of Petroleum Geologists, Tulsa, p. 239-248.
- Foster SSD (1987) Fundamental concepts in aquifer vulnerability, Pollution risk and protection strategy. In: Van Duijvenbooden W, Van Waegeningh HG (eds) *Vulnerability of soil and groundwater to pollutants*, Committee on hydrological research. The Hague, pp 69–86.

- Foster SSD, Hirata RCA, Gomes D, D'elia M, Paris M (2002) Quality protection groundwater: guide for water service companies. World Bank, Washington, DC, Municipal Authorities and Environment Agencies. <https://doi.org/10.1596/0-8213-4951-1>
- Gbaramatu-Voice Newspaper: 16th September 2021: 5
- George NJ, Nathaniel EU, Etuk SE (2014) Assessment of economical accessible groundwater reserve and its protective capacity in eastern Obolo local government area of Akwa Ibom State, Nigeria, using electrical resistivity method; *Int. J. Geophys.* 7(3) 693–700.
- George NJ, Aniekan M, Ekanem JI, Ibanga & Ndifreke I. Udosen (2017) Hydrodynamic Implications of Aquifer Quality Index (AQI) and Flow Zone Indicator (FZI) in groundwater abstraction: a case study of coastal hydro-lithofacies in South- eastern Nigeria. *J Coast Conserv* 21(4):759–776. <https://doi.org/10.1007/s11852-017-0535-3>
- George NJ (2021a) Modelling the trends of resistivity gradient in hydrogeological units: a case study of alluvial environment. *Model Earth Syst Environ* 7:95–104. <https://doi.org/10.1007/s40808-020-01021-3>
- George NJ (2021b) Geo-electrically and hydrogeologically derived vulnerability assessments of aquifer resources in the hinterland of parts of Akwa-Ibom State Nigeria. *Solid Earth Sci.* <https://doi.org/10.1016/j.sesci.2021.04.002>
- Gogu RC, Dassargues A (2000) Current trends and future challenges in groundwater vulnerability assessment using overlay and index methods. *Environ Geol* 39(6):549–559
- Heigold PC, Gilkeson RH, Cartwright K, Reed PC (1979) Aquifer transmissivity from surface electrical methods. *Groundwater* 17(4):338–345
- Henriet JP (1976) Direct application of Dar-Zarrouk parameters in groundwater survey; *Geophys. Prospect.* 24 344– 353.
- Khemiri S, Khnissi A, Alaya BA, Saidi S, Zargrouni F (2013) Using GIS for the comparison of intrinsic parameter methods assessment of groundwater vulnerability to pollution in scenarios of semiarid climate. The case of foussana groundwater in the central of Tunisia. *J. Water Resource Prot.* 5(8):835–845
- Kulke H (1995) Nigeria. In: Kulke, H., Ed., *Regional Petroleum Geology of the World, Part II, Africa, America, Australia and Antarctica*, Gebruder Borntraeger, Berlin, 143-172.
- Makeig KS (1982) National buffers for sludge leachate stabilization of groundwater; *Geophysics* 20(4) 420– 429.
- Merki PJ (1970) *Structural geology of the Cenozoic Niger Delta* (pp. 251–268). University of Ibadan Press, Ibadan.
- Nigeria Geological Survey Agency (2004) *Geological Map of Nigeria*. NGSA, Abuja.
- Obiora DN, Ajala AE, Ibuot JC (2015) Evaluation of aquifer protective capacity of overburden unit and soil corrosivity in Makurdi, Benue state, Nigeria, using electrical resistivity method. *J. Earth Syst. Sci.* 124(1) 125–135.
- Obiora DN, Ibuot JC (2020) Geophysical assessment of aquifer vulnerability and management: a case study of University of Nigeria, Nsukka, Enugu State. *Appl Water Sci* 10:29. <https://doi.org/10.1007/s13201-019-1113-7>

Publication of the European Centre for Research Training and Development -UK

- Okiotor ME, Eze SU, Owonaro JB, Saleh AS, Eriunu OM (2022) Evaluation of aquifer protective capacity and soilcorrosivity in Okerenkoko, Warri-southwest, Delta State, using one-dimensional resistivity inversion. Int'l journal of research and innovation in applied science (IJRIAS), (Vii), 48-55.
- Oladapo MI, Akintorinwa OJ (2007) Hydrogeophysical Study of Ogbese Southwestern, Nigeria. Global J Pure and Applied Sci. 2007; 13 (1): 55-61.
- Oladapo MI, Mohammed MZ, Adeoye OO, Adetola BA (2004) Geoelectrical investigation of the Ondo State Housing Corporation Estate, Ijapo Akure, Southwestern Nigeria. J Min Geol 40(1):41–48
- Olorunfemi MO, Olarewaju VO, Alade O (1991) “On the Electrical Anisotropy and Groundwater Yield in a Basement complex Area of S.W. Nigeria”, J. Afr. Earth Sci. 12(3):462-472.
- Olubusola IS, Adebo BA, Oladimeji OK, Daniel AA (2018) Application of GIS and Multi-Criteria Decision Analysis to Geoelectric Parameters for Modeling of Groundwater Potential around Ilesha, Southwestern Nigeria. European Journal of Academic Essays 5(5): 105-123.
- Oni TE, Omosuyi GO, Akinlalu AA (2017) Groundwater vulnerability assessment using hydrogeologic and geoelectric layer susceptibility indexing at Igbara-Oke, Southwestern Nigeria. NRIAG J Astron Geophys 6(2):452–458. <https://doi.org/10.1016/j.nrjag.2017.04.009>
- Rao BV, Briz-Kishore BH (1991) A methodology for locating potential aquifers in a typical semi-European Journal of Academic Essays 5(5): 105-123, 2018 123 arid region in India using resistivity and hydrogeologic parameters. Geoexploration”, 27, 55-64.
- Reynolds JM (1997) An introduction to applied and environmental geophysics. Wiley, Chichester, p 778
- Reyment RA (1965) Aspects of the Geology of Nigeria. University of Ibadan Press, Ibadan. p. 132.
- Rizka M (2018) Comparative studies of groundwater vulnerability assessment. IOP Conf Ser Earth Environ. Sci. 118(1):012018
- Short KC, Stauble AJ (1967) Outline of the geology of Niger Delta. Am Assoc Petrol Geol Bull, 51: 761– 779.
- Singh G, Singh J (2009) Water Supply and Sanitary Engineering. Delhi: Nem Chand Jain for Standard Publisher Distributors, 512 page.
- Stempvoort DV, Ewert L, Wassenaar L (1993) Aquifer vulnerability index: a GIS-compatible method for groundwater vulnerability mapping. Canad Water Resour J 18(1):25–37.
- Stigter TY, Ribeiro L, Carvalh AMM, Dill (2006) Evaluation of an intrinsic and a specific vulnerability assessment method in comparison with groundwater salinisation and nitrate contamination levels in two agricultural regions in the south of Portugal. Hydrogeol J 14(1–2):79–99. <https://doi.org/10.1007/s10040-004-0396-3>
- Surfer (2002) Contouring and 3D surface mapping for scientists and engineers. Golden software Incorporation, Colorado.

Publication of the European Centre for Research Training and Development -UK

- Ugbaja AN, Edet MO (2004) Groundwater pollution near shallow waste dumps in Southern Calabar, Nigeria; *Global J. Sci.* 2(2) 199–206.
- Ugwu NU, Ranganai RT, Simon RE, Ogubazghi G (2016) Geoelectric Evaluation of Groundwater Potential and Vulnerability of Overburden Aquifers at Onibu-Eja Active Dumpsite, Osogbo, Southwestern Nigeria. *J. of Water Res. And Protection*, 8, 311-329. <https://dx.doi.org/10.4236/jwarp.2016.83026>.
- Vander Velpen BPA (2004) WinRESIST Version 1.0. Resistivity sounding interpretation software. M.Sc. Research Project, ITC, Delft Netherland
- Vu T-D, Ni C-F, Li W-C, Truong M-H, Hsu SM (2021) Predictions of groundwater vulnerability and sustainability by an integrated index-overlay method and physical-based numerical model. *J Hydrol.* <https://doi.org/10.1016/j.jhydrol.2021.126082>